ORIGINAL PAPER

Average local ionization energy: A review

Peter Politzer · Jane S. Murray · Felipe A. Bulat

Abstract The average local ionization energy $\bar{I}(\mathbf{r})$ is the energy necessary to remove an electron from the point $\mathbf{r}$ in the space of a system. Its lowest values reveal the locations of the least tightly-held electrons, and thus the favored sites for reaction with electrophiles or radicals. In this paper, we review the definition of $\bar{I}(\mathbf{r})$ and some of its key properties. Apart from its relevance to reactive behavior, $\bar{I}(\mathbf{r})$ has an important role in several fundamental areas, including atomic shell structure, electronegativity and local polarizability and hardness. All of these aspects of $\bar{I}(\mathbf{r})$ are discussed.

Keywords Atomic shell structure · Average local ionization energy · Carbon nanotubes · Electronegativity · Local polarizability and hardness · Molecular reactivity

The concept of a local ionization energy

Chemical reactivity is local. It varies from one site in a molecule to another. In seeking to understand and predict reactive behavior, it is therefore important to be able to identify and rank the sites with the least strongly held, most available electrons as well as those where the electrons are tightly bound. This requires focusing not upon particular electronic orbitals, which are usually delocalized to some

extent, but rather upon specific points in the space of the molecule, even though electrons from several different orbitals may have a significant probability of being at each such point. It is for these reasons that the concept of an average local ionization energy, $\bar{I}(\mathbf{r})$, was introduced [1].

$\bar{I}(\mathbf{r})$ is defined in terms of the ionization energies of the electrons in individual molecular orbitals, and so we will begin with a discussion of these. First we want to mention, however, that the significance of $\bar{I}(\mathbf{r})$ is not limited to molecular reactivity. It has been found to be linked to local kinetic energy density, atomic shell structure, electronegativity, the electrostatic potential, and local polarizability and hardness. These fundamental aspects of $\bar{I}(\mathbf{r})$, as well as its applications in relation to chemical reactivity, will be examined in this paper. For earlier reviews, see Politzer and Murray [2, 3].

P. Politzer (✉) · J. S. Murray
CleveTheoComp,
1951 W. 26th Street, Suite 409,
Cleveland, OH 44113, USA
e-mail: ppolitze@uno.edu

F. A. Bulat
Naval Research Laboratory, Washington DC 20375,
under contract from Global Strategies Group (North America) Inc,
Crofton, MD 21114, USA

Electronic ionization energies

Within the Hartree-Fock framework, the ionization energy I_i of an electron in an orbital ϕ_i in an atom or molecule X can readily be determined simply by inserting the appropriate Hartree-Fock energy expressions into Eq. 1:

$$I_i = E(X_i^{+}) + E(e^{-}) - E(X), \tag{1}$$

$E(X)$ and $E(X_i^{+})$ are the energies of X and the positive ion formed by the loss of an electron from φ_i, the ith canonical Hartree-Fock orbital. This leads to,

$$I_i \approx |\varepsilon_i|, \tag{2}$$

where ε_i is the energy of an electron in φ_i. Equation 2 is based upon a major assumption: that the occupied orbitals of X are unaffected by the removal of an electron from φ_i.

Koopmans' theorem provides some support for this, by assuring the stability of ϕ_i itself [4, 5]. Nevertheless it is clearly unrealistic to treat the formation of the positive ion as unaccompanied by electronic/structural relaxation.

Equation 2 does benefit from a fortuitous partial cancellation of errors: The Hartree-Fock neglect of electronic correlation makes both $E(X_i^+)$ and $E(X)$ too high, but more so the latter because X has more electrons. However this is offset to some extent by not taking account of the relaxation of X_i^+, which increases $E(X_i^+)$. Thus Eq. 2 might be a reasonable approximation. When it is written for the highest-energy orbital in a molecule, it becomes,

$$I_1 \approx |\varepsilon_{HOMO}| \tag{3}$$

in which I_1 is the first ionization energy and ε_{HOMO} refers to the highest occupied molecular orbital (HOMO) energy.

How accurate are Eqs. 2 and 3? Eq. 3 is a reasonably satisfactory approximation. For a group of monosubstituted benzenes, we found the Hartree-Fock/6-31+G(d,p) $|\varepsilon_{HOMO}|$ to correlate well with experimental first ionization energies ($R^2=0.972$) and to be within about 0.1 eV of them [6]. For another set of 12 molecules of different types, the HF/6-31G(d) reproduce I_1 to within an average 0.7 eV [7]. For these molecules, the Hartree-Fock $|\varepsilon_i|$ are generally larger than the experimental I_i, and the deviations tend to be greater for the lower-lying valence orbitals, i.e., Eq. 2; the average absolute error is 0.9 eV for the two highest, but 2.2 eV for the lower ones. Increasing the basis set to 6–31+G(d,p) actually makes the results slightly worse.

We digress briefly here to mention that the procedure used to reach Eq. 3 is sometimes invoked to justify,

$$A \approx -\varepsilon_{LUMO} \tag{4}$$

where A is the molecule's electron affinity and ε_{LUMO} is the energy of the lowest unoccupied molecular orbital (LUMO). As pointed out by Cramer [8], the partial cancellation of errors that helps Eqs. 2 and 3 does not occur for Eq. 4; neglecting correlation and the relaxation of the negative ion that is formed *both* increase the energy of the latter relative to the neutral molecule, and the error in A is thereby amplified.

Returning to electronic ionization energies, the widespread utilization of Kohn-Sham density functional methodology [9, 10] makes it relevant to inquire as to the applicability of Eqs. 2 and 3 to Kohn-Sham orbital energies. There have been extensive theoretical analysis and discussion of this issue [11–20]. Janak's theorem [21] is often invoked to argue that Eqs. 3 and 4 are rigorously correct in *exact* Kohn-Sham theory, but that nothing is certain with regard to the other orbital energies; see, for example, Jellinek and Acioli [19]. Perdew and Levy

showed that the same conclusion can also be reached by another route [15]. A somewhat different viewpoint is that Eq. 2 is approximately valid for all Kohn-Sham orbital energies when computed at a sufficiently high level [13, 17, 18, 20]. Using very accurate Kohn-Sham potentials, Chong et al. found that the Kohn-Sham orbital energies approximate well the adiabatic ionization energies of the outer valence orbitals [17], a great improvement over Hartree-Fock and conventional density functional values. The connection between vertical ionization energies and occupied orbital energies is through the requirement that the Kohn-Sham and the exact electronic densities are identical, and is embodied primarily in the response term of the Kohn-Sham potential [22]. (This term was later used by Bulat et al. [23] to approximately relate Kohn-Sham average local ionization energies to those computed within Hartree-Fock theory.)

What is observed in general practice with respect to Kohn-Sham orbital energies? The general trend that we have found [6, 7], for three hybrid exchange/correlation functionals–B3PW91, B3LYP and B3P86–and two basis sets–6–31+G(d,p) and 6–311++G(3df,3pd)–is,

$$|\varepsilon_i|, \; Kohn-Sham < I_i, \; experiment < |\varepsilon_i|, \; Hartree-Fock \tag{5}$$

Depending upon the functional used, the Kohn-Sham $|\varepsilon_i|$ are 2–4 eV less than the corresponding I_i; this is true as well for ε_{HOMO}. For the monosubstituted benzenes mentioned above, Kohn-Sham B3P86/6–31+G(d,p), like Hartree-Fock, give a very good correlation with experimental I_1 ($R^2=0.968$), but are about 2 eV smaller in magnitude [6], probably due to the incorrect long-range behaviour of the exchange-correlation potential. For the 12 diverse molecules, the Kohn-Sham $|\varepsilon_i|$ are considerably below the measured I_i, but the deviations show a remarkable uniformity [7], for a given exchange/correlation functional. For B3PW91/6–31+G (d,p), for example, the error in 51 of the 57 estimated ionization energies, for the 12 molecules, is between 2.7 and 3.7 eV. In contrast, 43 of the 57 corresponding Hartree-Fock/6–31+G(d,p) errors are 0.5 to 3.5 eV, while the other 14 are even outside of this range.

The fact that the difference between I_i experimental and $|\varepsilon_i|$ Kohn-Sham is relatively constant (for a particular hybrid functional) has some significant consequences:

(1) It suggests that the discrepancy is largely systematic, perhaps indicating that the problem of electronic self-interaction has not been adequately addressed [24].
(2) The trends in the Kohn-Sham ε_i should be physically meaningful, perhaps more so than in the Hartree-Fock ε_i, which are more erratic with respect to the I_i.
(3) It should be possible to develop some general approach for converting the Kohn-Sham $|\varepsilon_i|$ into

better approximations of the experimental I_i. This has indeed been explored. Two straightforward procedures are to scale the Kohn-Sham $|\varepsilon_i|$ [25] or to add a constant term to them [26]. Another is to vary the parameters in Becke's hybrid exchange-correlation functional [27] so as to optimize a database of $|\varepsilon_i|$ with respect to the corresponding I_i [28]. For a more elaborate methodology, and additional discussion, see Jellinek and Acioli [19].

The average local ionization energy

If $\rho_i(\mathbf{r})$ is the electronic density of orbital $\varphi_i(\mathbf{r})$, having energy ε_i, and the total electronic density is $\rho(\mathbf{r})$, then the average orbital energy at the point $\mathbf{r}$ is,

$$\overline{\varepsilon}(\mathbf{r}) = \frac{\sum_i \rho_i(\mathbf{r})\varepsilon_i}{\rho(\mathbf{r})}. \tag{6}$$

The summation is over all occupied orbitals. If Eq. 2 is assumed to be valid, then Eq. 6 can be rewritten as,

$$\overline{I}(\mathbf{r}) = \frac{\sum_i \rho_i(\mathbf{r})|\varepsilon_i|}{\rho(\mathbf{r})}. \tag{7}$$

$\overline{I}(\mathbf{r})$ is the average local ionization energy at $\mathbf{r}$. The relationship of Eq. 6 to Eq. 7, which had been introduced earlier [1], was pointed out by Nagy et al. [29, 30]. The product of the orbital energy ε_i and its density $\rho_i(r)$ is a single-particle energy density; this is easily seen by multiplying the single-particle Hartree-Fock (or Kohn-Sham) equations by the complex conjugates of the orbital amplitudes [23]. Thus the numerators of both Eqs. 6 and 7 can be viewed as energy densities. Division by the total electronic density then yields an average–per electron–local ionization energy, Eq. 7.

As was explained in Sect. 1, $\overline{I}(\mathbf{r})$ was introduced as a guide to molecular reactivity. The straightforward rationale given above for Eq. 7 is fully consistent with this use of it, which shall be discussed in detail in a later section. It is noteworthy, however, that the expression on the right side of Eq. 7 has also appeared, quite some time ago but without any attention being drawn to it, in both Hartree-Fock [31] and Kohn-Sham [32] formalisms relating to local kinetic energy density, $t(\mathbf{r})$. Eq. 7 also appears naturally in computing the Kohn-Sham potential; for an example, see van Leeuwen and Baerends [33].

The kinetic energy density $t(\mathbf{r})$ is of interest in connection with kinetic energy functionals and also because it has been used to define local temperature, $T(\mathbf{r})$, by means of Eq. 8 [32],

$$t(\mathbf{r}) = \frac{3}{2}\rho(\mathbf{r})kT(\mathbf{r}) \tag{8}$$

in which k is the Boltzmann constant. More recently, Ayers et al. [34] and Bulat et al. [23] have explicitly linked $T(\mathbf{r})$ and $\overline{I}(\mathbf{r})$. For example, within the framework of Kohn-Sham theory, Bulat et al. obtained,

$$\frac{3}{2}kT(\mathbf{r}) + V(\mathbf{r}) + v_{XC}(\mathbf{r}) = -\overline{I}(\mathbf{r}). \tag{9}$$

In Eq. 9, $V(\mathbf{r})$ is the electrostatic potential at $\mathbf{r}$ due to the nuclei and electrons of the system:

$$V(\mathbf{r}) = \sum_A \frac{Z_A}{|\mathbf{R}_A - \mathbf{r}|} - \int \frac{\rho(\mathbf{r}')d\mathbf{r}'}{|\mathbf{r}' - \mathbf{r}|} \tag{10}$$

where Z_A is the charge on nucleus A, located at $\mathbf{R}_A$. The quantity $v_{XC}(\mathbf{r})$ in Eq. 9 is the exchange/correlation potential, the derivative of the exchange-correlation functional with respect to the electronic density. A notable feature of Eq. 9 is that it links two local properties–$\overline{I}(\mathbf{r})$ and $V(\mathbf{r})$–that are effective complementary indicators of molecular reactive behavior; this will be discussed in Sect. 7. An alternative way of writing Eq. 9, making use of Eq. 8, is

$$\frac{t(\mathbf{r})}{\rho(\mathbf{r})} + v_s(\mathbf{r}) = -\overline{I}(\mathbf{r}), \tag{11}$$

where we have collected all potential terms in $v_s(\mathbf{r})$. The average local ionization energy can therefore be viewed as what is needed to overcome the local excess of potential over kinetic energy.

As has been discussed on several occasions [30–35], $t(\mathbf{r})$ is not unambiguously defined, and therefore neither is $T(\mathbf{r})$. In deriving Eq. 9, Bulat et al. took $t(\mathbf{r})$ to be [23],

$$t(\mathbf{r}) = -\frac{1}{2} \sum_i \varphi_i^*(\mathbf{r})\nabla^2\varphi_i(\mathbf{r}). \tag{12}$$

Another possibility is [30],

$$t(\mathbf{r}) = \frac{1}{8} \sum_i \frac{\nabla\rho_i(\mathbf{r}) \cdot \nabla\rho_i(\mathbf{r})}{\rho_i(\mathbf{r})} - \frac{1}{8}\nabla^2\rho(\mathbf{r}) \tag{13}$$

or simply,

$$t(\mathbf{r}) = \frac{1}{8} \sum_i \frac{\nabla\rho_i(\mathbf{r}) \cdot \nabla\rho_i(\mathbf{r})}{\rho_i(\mathbf{r})}. \tag{14}$$

Note that all three definitions of $t(\mathbf{r})$ integrate to the same quantity, the system's kinetic energy. The choice is thus one of preference, although arguments have been given in favor of Eq. 14 [34] because it corresponds to a positive local kinetic energy density for all systems.

Nagy et al. have compared $\frac{3}{2}kT(\mathbf{r})$ and $\overline{I}(\mathbf{r})$ for several atoms (Be, C, O, Ne, Ar and Kr) and some first-row molecules (CO, O_2, CO_2, C_2H_2, C_2H_4 and HCN) [29, 30]; they used Eq. 13 to define $T(\mathbf{r})$. The quantities $\frac{3}{2}kT(\mathbf{r})$ and

$\bar{I}(\mathbf{r})$ were found to be of the same order of magnitude and showed, for the atoms, similar radial behavior, decreasing in a stepwise manner with increasing distance from the nucleus. Approximately parallel variations were observed in the molecules as well except in the directions perpendicular to the bonds at their midpoints, in which $\bar{I}(\mathbf{r})$ usually diminishes gradually while $\frac{3}{2}kT(\mathbf{r})$ has maxima and minima.

We end this section by mentioning a remarkable property of $\bar{I}(\mathbf{r})$: It is invariant to unitary transformations of the orbitals [23], although this would seem unlikely from its definition in terms of canonical orbitals, Eq. 7. This suggests a deeper relation between $\bar{I}(\mathbf{r})$ and the total electronic density $\rho(\mathbf{r})$, confirmed by the fact that within the Kohn-Sham formalism [through Eq. 9] it can be defined as a functional of $\rho(\mathbf{r})$ without explicit reference to orbitals.

Atomic shell structure

The preceding discussion leads in a natural manner to the important issue of shell structure in atoms, which is the basis for the periodicity in their properties. There have been extensive efforts to find a functional representation of shell structure, with some interesting results. Before going into these, we want to point out that there are really two issues here: (a) Can some criterion be established that places each shell boundary between the correct pair of atoms, *i.e.*, He/ Li, Ne/Na, *etc.*? (b) Will the integrated occupancies of the shells correspond to what is predicted by the periodic table? The focus of the work to be described has been upon issue (a); the occupancies generally begin to deviate from the expected values when the transition elements are encountered, even if (a) is satisfied, because the interpenetration of subshells becomes increasingly significant [36].

The electronic density of an atom, which we take to be spherically-averaged so that $\rho(\mathbf{r}) = \rho(r)$ [37], decreases monotonically with radial distance from the nucleus [38–40] and gives no indication of shell structure. The radial density, $4\pi r^2\rho(r)$, does go through maxima and minima [40–46], as does the Laplacian also, $\nabla^2\rho(r)$ [46–49]; most studies have found that the minima satisfactorily identify the K, L and L, M shell boundaries but not the subsequent ones. However Sen *et al.* have obtained shoulders in radial densities at the proper locations for the higher shell boundaries by using (a) numerical Hartree-Fock [44] and (b) Hartree [45] electronic densities. The latter study led to the conclusion that atomic shell structure has a purely electrostatic basis.

On the other hand, it has been demonstrated that shell structure is successfully reproduced, even for the heavy atoms, by functionals that involve $t(r)/\rho(r)$ [29, 31, 35, 50, 51]; $t(r)$ may be given, for example, by Eq. 11 or Eq. 13. Since $t(r)/\rho(r) \sim T(r)$, Eq. 8, this suggests a fundamental relationship between atomic shell structure and local temperature.

As noted in section 3, $\bar{I}(r)$ and $T(r)$ show similar behavior for atoms [29, 30]; thus it is to be expected that $\bar{I}(r)$ will also reflect shell structure. This was shown already in 1991 [52], without being aware of any link to $T(r)$ or $t(r)/\rho(r)$. When $\bar{I}(r)$ is plotted against radial distance from the nucleus, it decreases in a roughly stepwise fashion, with regions of slow and rapid variation alternating. This can be seen in Fig. 1 for neon, argon, krypton and xenon, computed with the numerical exact-exchange Kohn-Sham scheme of Talman and Shadwick [53, 54]. The inflection points in the radial plots of $\bar{I}(r)$ delineate the shells [see Fig. 1], usually quite accurately.

Finally, it is notable that the quantity $V(r)/\rho(r)$ also exhibits shell structure [55]. This is especially interesting because both $V(r)$ and $\rho(r)$ decrease monotonically from the nucleus [39], yet their ratio goes through maxima and minima, the former serving to indicate shell boundaries [55–57]. Sen *et al.* have labeled $V(r)/\rho(r)$ the average local electrostatic potential [56, 57].

$V(r)/\rho(r)$ plays a rather intriguing role in the analysis of atomic shell structure. Ghosh and Balbás used the Euler equation to show a connection between $V(r)/\rho(r)$ and the functional derivative of the kinetic energy [31]:

$$\frac{1}{\rho(\mathrm{r})}\frac{\delta T[\rho]}{\delta\rho} = -\frac{V(\mathrm{r})}{\rho(\mathrm{r})} + \frac{[\mu - \nu_{\mathrm{xc}}(\mathrm{r})]}{\rho(\mathrm{r})}. \qquad (15)$$

In Eq. 15, μ is the chemical potential. The quantity on the left side of Eq. 15, like $V(r)/\rho(r)$, shows shell structure [31]. However it has been observed [55] and later proven analytically [56] that the maxima of $V(r)/\rho(r)$ coincide with the minima of the radial density, $4\pi r^2\rho(r)$. Thus there is a link,
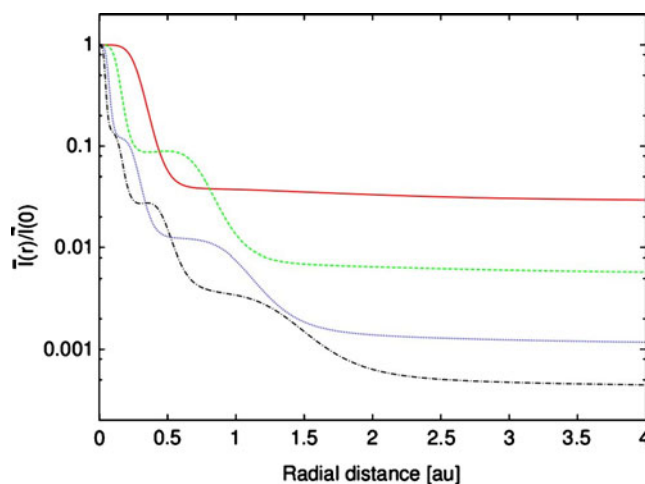

Fig. 1 Plot of (scaled) average local ionization energy against radial distance to the nucleus for atoms neon (red solid line), argon (green segmented line), krypton (blue dotted line), and xenon (black dotted-segmented line). The inflection points mark the boundaries between successive shells

through $V(r)/\rho(r)$, between the electronic density and the local kinetic energy approaches to atomic shell structure.

Electronegativity

The concept of electronegativity is certainly an important and very useful one, but unfortunately it does not pertain to a physical observable, and cannot be determined experimentally. Historically, the name of Pauling has been closely associated with electronegativity [58, 59], although the idea goes back at least to Berzelius, nearly a century earlier [60]. Pauling viewed electronegativity as "the power of an atom in a molecule to attract electrons to itself." [59], and he devised a scale of relative values based upon the estimated degrees of ionicity in heteronuclear covalent bonds.

Over the years, numerous other approaches to quantifying electronegativity have been proposed; these have been reviewed on several occasions [60–65]. The situation became such that Iczkowski and Margrave remarked, already in 1961, that "there is some confusion as to what physical picture corresponds to the term electronegativity" [66]. As they pointed out, there was not even agreement as to its units!

In 1978, Parr et al. sought to provide a rigorous basis for electronegativity (χ) by equating it to the negative of the electronic chemical potential μ [67]:

$$\chi = -\mu = -\left(\frac{\partial E}{\partial N}\right)_{\nu(\mathbf{r})}, \tag{16}$$

E is the electronic energy of an N-electron system in an external potential $\nu(\mathbf{r})$, which is usually that of the nuclei. An obvious issue with Eq. 16 is the validity of differentiating with respect to a quantity that can have only integral values [68, 69]. This has been addressed with considerable ingenuity [7, 70].

Equation 16 can be converted into a more tractable expression for χ by making one of three assumptions [65, 70–74]:

(a) The derivative in Eq. 15 can be treated by a finite-difference approximation.
(b) E is a quadratic function of N.
(c) E(N) can be expanded as a Taylor series around N_0, the number of electrons in the ground-state system, and truncated after the second-order term.

Any one of these assumptions, which have been analyzed elsewhere [65, 73, 74], will lead to,

$$\chi \approx 0.5(I_1 + A) \tag{17}$$

As in Sect. 2, I_1 and A are the first ionization energy and the electron affinity of the system. Since Eq. 16 stipulates that $\nu(\mathbf{r})$ should be held constant, the vertical I_1 and A should be used in Eq. 17; however this restriction is often ignored and adiabatic values are inserted. This is an important point; only if $\nu(\mathbf{r})$ is constant is it valid to treat E as a function of N alone [67]. Electronegativities obtained with Eq. 17 and measured I_1 and A are sometimes described as "experimental values." This is wrong; electronegativity is not a physical observable, no matter what the sources of the data from which it is calculated.

Equation 17 is commonly applied to molecules as well as to atoms, which poses another problem: what is meant by the electronegativity of a molecule? It is certainly far afield from how Pauling and his contemporaries as well as many current experimentalists understand the term, as focusing upon an interacting atom. It can indeed be argued, as have Pearson [75] and Allen [76], that there should be separate scales for χ and μ. (There is no problem with extending μ to molecules.)

There is also the practical issue with Eq. 16 that it gives some electronegativities that are greatly at variance with chemical experience. For example, some relative values predicted by Eq. 17 are: Cl > O, Cl >> N, Br ~ O and Br > N [70].

Allen et al. have introduced an atomic property, now called the "configuration energy" (CE), which was proposed as a measure of electronegativity [77–79]. The CE is the average ionization energy of the valence electrons of the free atom; thus, for the non-transition elements,

$$CE = \frac{n_s \varepsilon_s + n_p \varepsilon_p}{n_s + n_p}. \tag{18}$$

In Eq. 18, n_s and n_p are the numbers of s and p valence electrons and ε_s and ε_p are the differences in the multiplet-averaged total energies of the atom and its appropriate positive ion in their ground states, to be obtained spectroscopically.

The CE resulting from Eq. 18 were shown to be consistent with various physical and chemical properties [77], and to correlate well with up-dated Pauling electronegativities [80] as well as the well-regarded ones of Allred and Rochow [81]. In extending Eq. 17 to transition elements, however, identifying the valence electrons can become ambiguous [78, 79] and there is the problem of interpenetration of subshells [36] (which can also be significant for non-transition elements).

We have shown that these problems can be avoided, while still remaining true to Allen's concept, by working in terms of the average local ionization energy [82]. $\bar{I}(\mathbf{r})$ is constant on any spherically-averaged surface of an atom [37], and if that surface is sufficiently far from the nucleus, then–as per section $2 - \bar{I}(r)$ will be an approximation to the average ionization energy of the valence electrons, i.e., Allen's configuration energy, CE.

Bader *et al.* have proposed that the surface of an atom or molecule can reasonably be taken to be the 0.001 au (electrons/bohr^3) contour of its electronic density [83]; this typically encompasses roughly 98% of its electronic charge. As was discussed in the preceding section, $\bar{I}(r)$ does delineate the boundaries of atomic shells [52], and the radii of the $\rho(r) = 0.001$ au surfaces confirm that they fall within the outermost (valence) shells [82]. We use the label $\overline{I_S}(r)$ for $\bar{I}(\mathbf{r})$ computed on the surface of an atom or molecule.

When the $\overline{I_S}(r)$ on the $\rho(r) = 0.001$ au surfaces of the atoms H–Kr were plotted against Allen's CE, the R^2 was 0.976 for the non-transition elements [82]. As mentioned above, the transition elements pose problems for Allen's methodology [78, 79]. When they were included in the correlation, R^2=0.959 [82].

We suggest that the $\overline{I_S}(r)$ on $\rho(\mathbf{r}) = 0.001$ au atomic surfaces provide an easily-determined and effective measure of relative electronegativities. It has the good feature of Allen's approach, in accord with chemical experience, but (a) there is no need to identify and enumerate valence electrons, and (b) since $\overline{I_S}(r)$ is obtained by summing over all occupied orbitals, any interpenetration of subshells is automatically taken into account.

Local polarizability/hardness

Polarizability, hardness and charge capacity are closely-related properties, and are in turn linked to electronegativity. However only polarizability (α) is a physical observable; it is a tensor quantity that determines (to first order) how a charge distribution will be affected (polarized) by an external electric field ε [84, 85]. Specifically, a dipole moment will be induced, given by,

$$\mu_{ind} = \alpha \cdot \varepsilon. \tag{19}$$

In the present context, our interest is in the scalar (average) polarizability, obtained by diagonalizing the 3×3 Cartesian tensor matrix:

$$\alpha = \langle \boldsymbol{\alpha} \rangle = \frac{1}{3}\left(\alpha_{xx} + \alpha_{yy} + \alpha_{zz}\right). \tag{20}$$

Polarizability is of fundamental importance in both covalent and noncovalent interactions, although it is sometimes invoked under other names. For example, in 1963 Pearson introduced the hard/soft acid/base theory as an empirical means of rationalizing a great deal of known reactive behavior [86, 87]. Hardness and softness simply correspond to low and high polarizability, respectively. Also in the mid-1960s, Huheey was developing the concept of charge capacity, which is a measure of how much an atom's electronegativity changes as it gains or loses electronic charge in the process of forming a molecule

[88, 89]. The charge capacity indicates how well an atom adapts to gaining or losing electronic charge–which reflects its polarizability. Correlations and explicit relationships between polarizability, hardness/softness, and charge capacity have indeed been developed [74, 90–94]. The greater is the polarizability, the greater is the charge capacity and the lower is the hardness. It should be noted that polarizability and hardness are readily applicable to molecules and chemical groups as well as atoms, while charge capacity was established in the context of groups and atoms. Since charge capacity and hardness are essentially the inverse of each other [74, 90], the following discussion will focus only upon polarizability and hardness.

How does the average local ionization energy come into this? It is long known that polarizability correlates well with volume, $\alpha \sim V$, for both atoms and molecules [95–100]. For atoms (but not molecules), it has also been shown to be inversely related to the first ionization energy [52, 97, 101, 102], although this may simply reflect the inverse variation of I_1 with atomic size.

However since it is the least tightly-held electrons that are most affected by an electric field (*i.e.*, are most polarizable) [103, 104], it seems reasonable that polarizability in general should depend at least to some extent upon ionization energy. This has been confirmed. For a representative group of 29 molecules, the $\alpha \sim V$ correlation had R^2=0.960; this improved to 0.984 when the average value of $\overline{I_S}(\mathbf{r})$ on the $\rho(\mathbf{r}) = 0.001$ au molecular surface was introduced: $\alpha \sim V/\bar{I}_{S,ave}$ [100]. The root-mean-square error decreased from 0.76 to 0.48 Å^3. We have further demonstrated that the quantity $V/\bar{I}_{S,ave}$ can be used to estimate the polarizabilities α_i of components of molecules, *e.g.*, atoms and groups [105, 106]. These can then be combined to predict molecular values,

$$\alpha \approx \sum_i \alpha_i. \tag{21}$$

Polarizability is not uniform throughout a molecule. As mentioned above, the most loosely-held electrons are expected to be the most polarizable [103, 104], *e.g.* π electrons and lone pairs. We have proposed that the average local ionization energy $\bar{I}(\mathbf{r})$ be viewed as an inverse measure of local polarizability $\alpha(\mathbf{r})$ [52, 100, 107]; the higher is $\bar{I}(\mathbf{r})$, the lower is $\alpha(\mathbf{r})$. The volume of the overall system should now not be a factor, because only equal increments of volume, $d\mathbf{r}$, are being compared. Evidence supporting an inverse $\alpha(\mathbf{r}) - \bar{I}(\mathbf{r})$ relationship has been presented [100]; for example, the regions of lowest $\bar{I}(\mathbf{r})$ in a group of molecules coincide with the largest components of their experimental polarizabilities.

Proceeding to hardness η, this was originally introduced by Pearson as an empirical concept [86, 87].

However he and Parr later gave it a quantitative form [108]:

$$\eta = \frac{1}{2} \left(\frac{\partial^2 E}{\partial N^2} \right)_{v(\mathbf{r})}. \tag{22}$$

Analogously to χ (or μ), this can be converted to,

$$\eta = 0.5(I_1 - A) \tag{23}$$

by making one of the three assumptions given in relation to Eq. 16. Equations 22 and 23 face the same issues as do Eqs. 16 and 17, except that hardness (and chemical potential) can be extended to molecules with no conceptual difficulty, unlike electronegativity. However the evaluation of molecular hardness *via* Eq. 23 can be questioned [69]. We have accordingly proposed an alternative route to quantifying hardness, in terms of polarizability–which in turn will lead to the average local ionization energy!

Hardness has been linked inversely to polarizability ever since the former was introduced [70, 86, 87, 90–94]. However, while η calculated by Eq. 23 does correlate with α for atoms, $\eta \sim \alpha^{-1/3}$ ($R^2 = 0.868$) [73], this is much less the case for molecules ($R^2 = 0.684$) [74].

We have suggested that hardness be formulated in terms of an inverse cubic relationship with polarizability, but using $V/\bar{I}_{S,ave}$ for the latter (shown above to be an effective representation of α). Thus, our operational definition of relative hardness is [74],

$$\eta^{rel} = \left[\frac{\bar{I}_{S,ave}}{V} \right]^{1/3}. \tag{24}$$

Just as with polarizability, Eq. 24 allows relative hardnesses η_i to be determined for components of molecules. Then a molecular value can be obtained by,

$$\eta^{rel} = \left[\sum_i \left(\frac{1}{\eta_i^{rel}} \right)^3 \right]^{-1/3}. \tag{25}$$

Reactivity

We come now to the use of $\bar{I}(\mathbf{r})$ in analyzing and predicting reactive behavior. For this purpose it is normally computed on the surface of the molecule of interest, *i.e.*, $\bar{I}_S(\mathbf{r})$ [109], since this is what an approaching reactant encounters. Examples of $\bar{I}_S(\mathbf{r})$ computed with the WFA code and Surface Analysis Suite [109] at the B3PW91/6–31G(d,p) level (unless otherwise stated) are shown in Figs. 2, 3, 4 and 5, and will be discussed in this section. The surface is typically taken to be the 0.001 au contour of $\rho(\mathbf{r})$ [83], but the qualitative features of $\bar{I}_S(\mathbf{r})$ are the same for other outer

contours of $\rho(\mathbf{r})$ [1, 6, 109]. Of primary interest are the magnitudes and locations of the lowest values of $\bar{I}_S(\mathbf{r})$, the local minima $\bar{I}_{S,min}$. These reveal the least tightly-held, most reactive electrons, which should be the sites most vulnerable to electrophilic or to free radical attack. Overall, these expectations have been confirmed, as shall be seen. (There are some indications that the local maxima of $\bar{I}_S(\mathbf{r})$ may play an analogous role with respect to nucleophiles [109], but this needs to be further investigated.)

Another local property that has often been used in relation to reactivity is the electrostatic potential $V(\mathbf{r})$, defined by Eq. 10 [110–113], and related to $\bar{I}(\mathbf{r})$ through Eq. 9. In this context, it is also frequently evaluated on the molecular surface, *i.e.*, $V_S(\mathbf{r})$ [109]. It is the most negative and the most positive $V_S(\mathbf{r})$, the $V_{S,min}$ and $V_{S,max}$, that are relevant to the approach of electrophiles and nucleophiles, respectively.

Reaction with an electrophile can involve several factors, and it may sometimes not be possible to characterize it in terms of a single descriptor. Acid/base behavior is a good example. This involves the interaction of a base with a proton; therefore it is the $\bar{I}_{S,min}$ and $V_{S,min}$ of the basic site that are relevant. For instance, to correlate and predict the pK_a of a group of carboxylic acids, R-COOH, what is needed are the $\bar{I}_{S,min}$ and $V_{S,min}$ of the carboxylate anions, R-COO$^-$. Apart from any structural changes, two key factors are (a) the electrostatic attraction between the proton and the base, which is indicated by the $V_{S,min}$ of the latter, and (b) how readily can the base share electronic charge with the proton, *i.e.*, the $\bar{I}_{S,min}$ of the base. The more negative is $V_{S,min}$ and the lower is $\bar{I}_{S,min}$, the stronger will be the base-H$^+$ interaction and hence the less acidic will be the conjugate acid and the higher its pK_a.

When comparing basic sites that are in the same row of the periodic table (corresponding, for example, to carbon or nitrogen acids, carboxylic and other oxoacids, azines, azoles, *etc.*), the $V_{S,min}$ are likely to be roughly similar, and so the $\bar{I}_{S,min}$ are the dominant factor. It is then possible to obtain good correlations between $\bar{I}_{S,min}$ and pK_a, protonation enthalpy and substituent constants (*e.g.*, Hammett, Taft) [114–116]. When the basic sites are in different rows, however, $V_{S,min}$ becomes markedly less negative with the significant increases in atomic size (especially first to second row), which is in accord with the increasing acidity, while $\bar{I}_{S,min}$ changes relatively little [117]. For instance, it is $V_{S,min}$ that correctly predicts the pK_a to decrease in going from H_2O to H_2S to H_2Se. It is accordingly necessary to take both $\bar{I}_{S,min}$ and $V_{S,min}$ into account. For the nine hydrides in the first three rows of Groups V–VII, both pK_a and enthalpy of protonation were found to be expressed well by relationships of the form of Eq. 26 [117], in which $\bar{I}_{S,min}$ and $V_{S,min}$ play complementary roles.

$$pK_a \left(or\ \Delta H_{prot} \right) = \alpha \bar{I}_{S,min} + \beta V_{S,min} + \gamma. \tag{26}$$

However when the focus is upon a single type of basic site in different molecular environments, as in correlating the pK_a of variously-substituted anilines [118] or phenols (i.e., phenolate anions [119]), then either $\bar{I}_{S,min}$ or $V_{S,min}$ is sufficient.

On the other hand, for electrophilic attack on mono-substituted benzene derivatives, C_6H_5X, it is only $\bar{I}_S(\mathbf{r})$ that is reliable [1, 6, 116, 120]. $V_S(\mathbf{r})$ can be quite misleading. The most negative $V_{S,min}$ is frequently near the substituent X (e.g., when X = NH_2, OH, F, Cl, NO_2 [120]), with a weaker negative $V_S(\mathbf{r})$ above and below the ring. The latter is due to the π electrons and does not favor any particular carbon. $V_S(\mathbf{r})$ therefore incorrectly predicts interaction with an electrophile to occur at X. In contrast, the lowest $\bar{I}_{S,min}$ are associated with the ring carbons, and are fully consistent with the known ortho-and para-or meta-directing tendencies of each substituent [1, 6, 116, 120]. This can be seen very clearly in the computed $\bar{I}_S(\mathbf{r})$ for anisole (X= OCH_3) and benzoic acid (X=COOH) in Fig. 2. ($\bar{I}_S(\mathbf{r})$ is even in agreement with the unusual meta/para combination observed for the NH_3^+ group [1].) Furthermore, comparison with the carbon $\bar{I}_{S,min}$ of benzene indicates correctly in each case whether the substituent activates or deactivates the ring toward electrophilic substitution. For example, the $\bar{I}_{S,min}$ of anisole and benzoic acid, shown in Fig. 2, are 0.4 eV less and greater, respectively, than that of benzene.

Thus, while electrostatics may initially draw an electrophile to X, the energetics of electron transfer are determining and dictate that reaction will occur at the ring carbons. An exception is aniline, in which the NH_2 has an $\bar{I}_{S,min}$ comparable to those of the ring carbons [4], and protonation of the nitrogen has indeed been observed [121]. In some instances, such as furan and pyrrole, the function of the negative $V_S(\mathbf{r})$ appears to be to bring the electrophile into

the vicinity of the site with the lowest $\bar{I}_{S,min}$ [120], another example of $\bar{I}_S(\mathbf{r})$–$V_S(\mathbf{r})$ complementarity. Heterocyclic molecules are discussed in greater detail by Bulat et al. [122]. A particularly noteworthy finding is that in some instances the site of the lowest $\bar{I}_{S,min}$ in a molecule (most often nitrogen-containing) is not associated with the HOMO. This underscores the limitations of the frontier molecular orbital approach to reactivity, and the advantage of $\bar{I}_S(\mathbf{r})$ in that it considers contributions from all of the occupied orbitals. (Note, also, that a link between $\bar{I}(\mathbf{r})$ and the Fukui function has been discussed [123].)

$\bar{I}_{S,min}$ are not limited to atomic sites; they are also associated with localized buildups of electronic charge in bond regions. Thus there are $\bar{I}_{S,min}$ above and below the midpoint of the double bond in ethylene [124], but not the C-C bonds in benzene, in which the π electrons are delocalized [1, 6, 120]. Good examples are the polycyclic aromatic hydrocarbons, such as the infamous carcinogen benzo[a]pyrene (1). It has long been recognized that the C-C bonds in these molecules are not all equivalent [125]. This can be seen from the crystallographic C-C bond lengths; for a given molecule, these cover a range of 0.1 Å or more, between approximately 1.35 and 1.45 Å [126]. For comparison, the C-C distances in ethylene and in benzene are 1.339 and 1.399 Å, respectively [80]. There are invariably $\bar{I}_{S,min}$ above and below the shortest C-C bonds in the polycyclic aromatic hydrocarbons [126], reflecting their near-double-bond characters. In **1**, they are, as indicated by dots, above and below bonds 1–2, 6–7, 9–10, 11–12 and 16–20. The lowest of these $\bar{I}_{S,min}$ are those of bonds 1–2 and 6–7, as can be seen very clearly in Fig. 3; these were formerly labeled K regions, and were viewed as relatively electron-rich reaction centers involved in tumorigenesis [127–129].
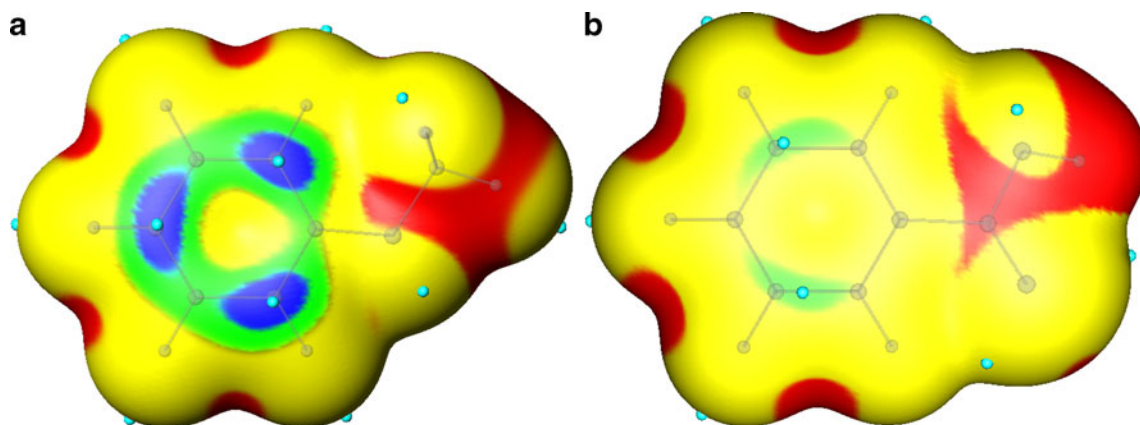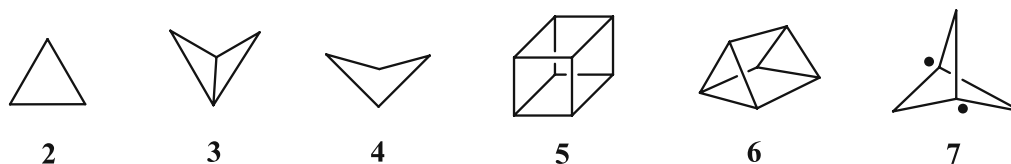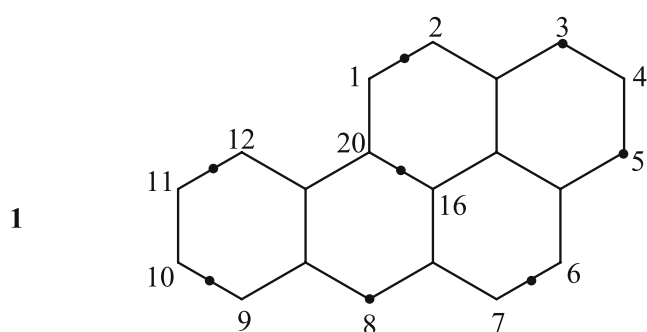

Fig. 2 Average local ionization energy on the molecular surfaces of (**a**) anisole and (**b**) benzoic acid. The colors correspond to the following range of values, in eV: Red > 12.4 > Yellow > 9.7 > Green >9.1 > Blue. The light blue dots on the molecular surface indicate the locations of the $\bar{I}_{S,min}$. The lowest $\bar{I}_{S,min}$ for anisole and benzoic acid have values of 8.8 and 9.6 eV, respectively

These observations are relevant to the past controversy as to whether there is a bond between the two central carbons in [1, 1, 1]propellane **7** [133, 134]. If there were, then the molecule would have three three-membered rings, and the C-C bonds would be expected to have $\overline{I}_{S,min}$. However the only $\overline{I}_{S,min}$ found are to the outsides of the central carbons, as shown in the structural drawing of **7** and Fig. 4b. This supports our earlier argument that there is no central C-C bond, and that the molecule instead has biradical character [135], for which experimental evidence is cited.

This brings us back to the polycyclic aromatic hydrocarbons, in which there are also $\overline{I}_{S,min}$ by some of the

Consistent with $\overline{I}_{S,min}$ being associated with double bond character is that they are found near the midpoints of the strained C-C bonds in three-membered rings of hydrocarbons, e.g., **2** [shown in Fig. 4a] and **3** [124]; these bonds are known to have some olefin-like reactive properties [130–133]. However the C-C bonds in four-membered hydrocarbon rings (e.g., **4** and **5**) do not have $\overline{I}_{S,min}$ [124]. In **6**, the bonds at the ends which are parts of three-membered rings do, but the connecting ones do not.

carbons [126], e.g., positions 3, 5 and 8 in benzo[a]pyrene, **1**; see Fig. 3. We again interpret them as denoting some degree of radical character, which agrees with a variety of laboratory observations. For instance, NMR analyses show carbons 3, 5 and 8 to be the most reactive in **1** [136]; they are known to be the sites of quinone formation [137].

From polycyclic aromatic hydrocarbons, it is a short step to graphene and then to carbon nanotubes, which can be viewed as graphene rolled up in various ways [138–140]. $\overline{I}_S(\mathbf{r})$ has been computed for graphene [141] and for different carbon nanotubes [142–144], as well as some other compositions [142, 143]. In general, there is an $\overline{I}_{S,min}$ above each carbon, as in benzene. However the magnitudes tend to be lower for carbon nanotubes than for benzene or graphene, indicating that the curvatures of the tubes increase reactivity. For a (5,5) carbon nanotube with a Stone-Wales defect (in which four carbon hexagons are replaced by two 5-membered-and two 7-membered rings), the $\overline{I}_{S,min}$ have been shown to correlate with computed hydrogen and fluorine atom chemisorption energies at the various carbon sites [144]. The most reactive carbons are those shared by 5-, 6-and 7-membered rings.

A remarkable feature of (n,0) carbon nanotubes in particular is their ability to transmit electronic perturbations throughout their lengths [143, 145, 146]. This has been observed for both $\overline{I}_S(\mathbf{r})$ and $V_S(\mathbf{r})$: seemingly small perturbations at one end propagate through the tube and result in striking gradations of both of these properties along the tube's length. The rather weak $V_S(\mathbf{r})$ and uniformly grid-like $\overline{I}_S(\mathbf{r})$ of unsubstituted (hydrogen terminated) carbon nanotubes [147, 148] change dramatically upon substitution at either (or both) ends [143, 145, 146,
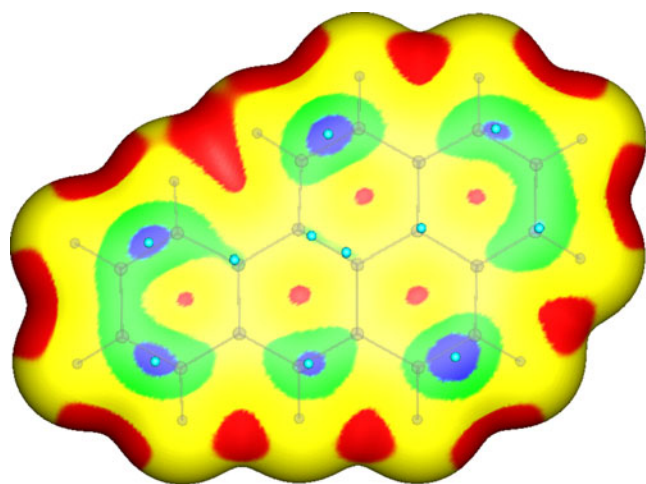

Fig. 3 Average local ionization energy on the molecular surface of benzo[a]pyrene (1). The colors correspond to the following range of values, in eV: Red > 11.8 > Yellow > 9.8 > Green > 9.1 > Blue. The light blue dots on the molecular surface indicate the locations of the $\overline{I}_{S,min}$ with values smaller than 10.0 eV
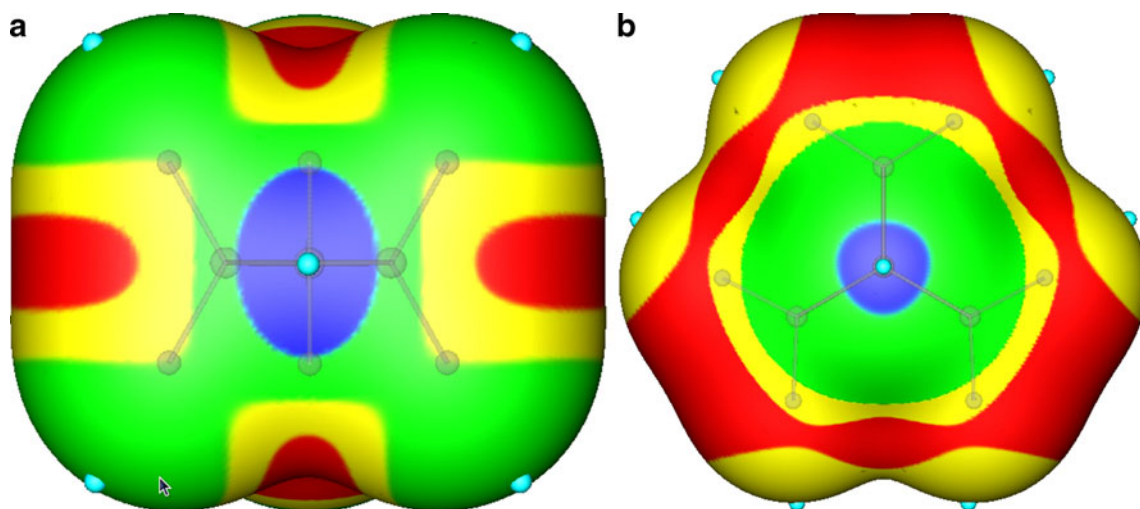
Fig. 4 Average local ionization energy on the molecular surfaces of (**a**) cyclopropane (2) and (**b**) propellane (7). The colors correspond to the following range of values, in eV: (**a**) Red > 12.0 > Yellow > 11.5 > Green > 10.9 > Blue. (**b**) Red > 12.0 > Yellow > 11.0 > Green > 8.0 > Blue. The light blue dots on the molecular surfaces indicate the locations of the $\overline{I}_{S,min}$. The view of cyclopropane is through the axis joining the midpoint of one C-C bond and the third C atom, with the latter going into the paper; the $\overline{I}_{S,min}$ seen in the blue region is along one of the strained C-C bonds. Propellane is shown through the axis joining the two central carbon atoms; the $\overline{I}_{S,min}$ seen in the blue region is associated with one of these central carbons

149]. For example, replacing one terminal hydrogen atom by an NH_2 group results in rather low $\overline{I}_S(\mathbf{r})$ values at that end, with the perturbation propagating through the tube and leading to higher values at the opposite end, as seen in Fig. 5. For the electrostatic potential, analogous behavior is observed. This characteristic of (n,0) nanotubes has been related to the fact that they alone possess a large number of bonds parallel to the tube axis.

Summary

In this review, we have sought to convey an appreciation of the various significant aspects of the average local ionization energy, $\overline{I}(\mathbf{r})$. It is linked to the kinetic energy

density and is able to reproduce atomic shell structure; it is an effective measure of electronegativity, and provides a means of quantifying local polarizability and hardness. These features underscore the fundamental role of $\overline{I}(\mathbf{r})$ as a descriptor of electronic behavior. Finally, $\overline{I}_S(\mathbf{r})$ is, in conjunction with the electrostatic potential, a very useful guide to molecular reactivity. An indication of the growing recognition of the importance of $\overline{I}(\mathbf{r})$ is its increasing incorporation into software packages, e.g. the WFA Surface Analysis Suite [109].

We concluded our previous review of $\overline{I}(\mathbf{r})$ with the statement "Thus, there remains much to be investigated!" [3]. As with any active and productive research area, that statement continues to be true. The fact that $\overline{I}(\mathbf{r})$ can be expressed as a functional of the electronic density, with no

Fig. 5 Average local ionization energy on the molecular surface of a 3-unit cell (6,0) carbon nanotube substituted on one end (left) with an NH_2 group. The colors correspond to the following range of values, in eV: Red > 18.0 > Yellow > 14.0 > Green > 11.7 eV > Blue. The wave-function was obtained at the HF/6–31G(d) level. Light blue dots on the molecular surface indicate the locations of the lowest $\overline{I}_{S,min}$: minima **a**, **b**, **c**, **d** (on C1, C2, C3, and C4) at ~8.5 eV, and minimum **e** (on C5) at ~7.5 eV)
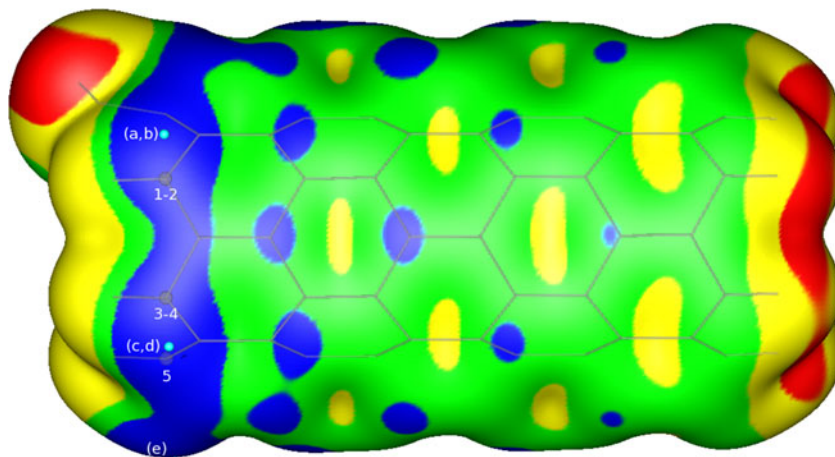
reference to orbitals, is intriguing and needs to be pursued. (In this context, it is noteworthy that Ayers and Nagy included $\bar{I}(\mathbf{r})$ among possible alternatives to the electronic density as fundamental descriptors of Coulomb systems [150].) Can $\overline{I_S}(\mathbf{r})$ be a diagnostic for nonlinear optical activity in carbon nanotube systems? Can $\overline{I_S}(\mathbf{r})$ be a reliable indicator of sites for nucleophilic attack? These (and other) ideas and questions confirm that there does indeed still remain much to be investigated.

References

1. Sjoberg P, Brinck T, Murray JS, Politzer P (1990) Can J Chem 68:1440–1443
2. Murray JS, Politzer P (1996) In: Parkanyi C (ed) Theoretical organic chemistry. Amsterdam, Elsevier
3. Politzer P, Murray JS (2007) In: Toro-Labbé A (ed) Chemical reactivity. Amsterdam, Elsevier, Ch 8
4. Nesbet RK (1965) Adv Chem Phys 9:321–363
5. Koopmans TA (1934) Physica 1:104–113
6. Politzer P, Abu-Awwad F, Murray JS (1998) Int J Quantum Chem 69:607–613
7. Politzer P, Abu-Awwad F (1998) Theoret Chem Acc 99:83–87
8. Cramer CJ (2002) Essentials of computational chemistry. Wiley, New York
9. Hohenberg P, Kohn W (1964) Phys Rev 136:B864–B871
10. Kohn W, Sham LJ (1965) Phys Rev 140:A1133–A1138
11. Perdew JP, Parr RG, Levy M, Balduz JL Jr (1982) Phys Rev Lett 49:1691–1694
12. Levy M, Perdew JP, Sahni V (1984) Phys Rev A 30:2745–2748
13. Krieger JB, Li Y, Iafrate GJ (1992) Phys Rev A 45:101–126
14. Kleinman L (1997) Phys Rev B 56:12042–12045, 16029–16030
15. Perdew JP, Levy M (1997) Phys Rev B 56:16021–16028
16. Harbola MK (1999) Phys Rev B 60:4545–4550
17. Chong DP, Gritsenko OV, Baerends EJ (2002) J Chem Phys 116:1760–1772
18. Hamel S, Casida ME, Salahub DR (2002) J Chem Phys 116:8276–8291
19. Jellinek J, Acioli PH (2003) J Chem Phys 118:7783–7796
20. Gritsenko OV, Braïda B, Baerends EJ (2003) J Chem Phys 119:1937–1950
21. Janak JF (1978) Phys Rev B 18:7165–7168
22. Baerends EJ, Gritsenko OV (1997) J Phys Chem A 101:5383–5403
23. Bulat FA, Levy M, Politzer P (2009) J Phys Chem A 113:1384–1389
24. Perdew JP, Norman MR (1982) Phys Rev B 26:5445–5450
25. Stowasser R, Hoffmann R (1999) J Am Chem Soc 121:3414–3420
26. Akola J, Manninen M, Häkkinen H, Landman U, Li X, Wang L-S (1999) Phys Rev B 60:R11297–R11300
27. Becke AD (1993) J Chem Phys 98:5648–5652
28. Politzer P, Abu-Awwad F (2000) J Comput Chem 21:227–238
29. Nagy Á, Parr RG, Liu S (1996) Phys Rev A 53:3117–3121
30. Gál T, Nagy Á (1997) Mol Phys 91:873–880
31. Ghosh SK, Balbás LC (1985) J Chem Phys 83:5778–5783
32. Ghosh SK, Berkowitz M, Parr RG (1984) Proc Natl Acad Sci USA 81:8028–8031
33. van Leeuwen R, Baerends EJ (1994) Phys Rev A 49:2421–2431
34. Ayers PW, Parr RG, Nagy Á (2002) Int J Quantum Chem 90:309–326
35. Navarrete-López AM, Garza J, Vargas R (2008) J Chem Phys 128:104110 (1–8)
36. Politzer P, Daiker KC (1973) Chem Phys Lett 20:309–316
37. Delgado-Barrio G, Prat RF (1975) Phys Rev A 12:2288–2297
38. Sperber G (1971) Int J Quantum Chem 5:189–214
39. Weinstein H, Politzer P, Srebrznik S (1975) Theor Chim Acta 38:159–163
40. Simas AM, Sagar RP, Ku ACT, Smith VH Jr (1988) Can J Chem 66:1923–1930
41. Politzer P, Parr RG (1976) J Chem Phys 64:4634–4637
42. Boyd RJ (1976) J Phys B 9:L69–L72
43. Boyd RJ (1977) J Chem Phys 66:356–358
44. Sen KD, Slamet M, Sahni V (1993) Chem Phys Lett 205:313–316
45. Sahni V, Qian Z, Sen KD (2001) J Chem Phys 114:8784–8788
46. Eickerling G, Reiher M (2008) J Chem Theory Comput 4:286–296
47. Sagar RP, Ku ACT, Smith VH Jr, Simas AM (1988) J Chem Phys 88:4367–4374
48. Shi Z, Boyd RJ (1988) J Chem Phys 88:4375–4377
49. Kohout M, Savin A, Preuss H (1991) J Chem Phys 95:1928–1942
50. Kohout M, Savin A (1996) Int J Quantum Chem 60:875–882
51. Pacios LF, Gómez PC (1998) J Comput Chem 19:488–503
52. Politzer P, Murray JS, Grice ME, Brinck T, Ranganathan S (1991) J Chem Phys 95:6699–6704
53. Talman JD, Shadwick WF (1976) Phys Rev A 14:36–40
54. Talman JD (1989) Comput Phys Commun 54:85–94
55. Politzer P (1980) J Chem Phys 72:3027–3033
56. Sen KD, Gayatri TV, Krishnaveni R, Kakkar M, Toufar H, Janssens GOA, Baekelandt BG, Schoonheydt RA, Mortier WJ (1995) Int J Quantum Chem 56:399–408
57. Sen KD, Gayatri TV, Toufar H (1996) J Mol Struct THEOCHEM 361:1–13
58. Pauling L (1932) J Am Chem Soc 54:3570–3582
59. Pauling L (1942) The nature of the chemical bond, 2nd edn. Cornell University Press, Ithaca
60. Hinze J (1999) In: Maksic ZB, Orville-Thomas WJ (eds) Pauling's Legacy. Modern Modelling of the Chemical Bond. Elsevier, Amsterdam, pp 189–212
61. Pritchard HO, Skinner HA (1955) Chem Rev 55:745–786
62. Ferreira R (1967) Adv Chem Phys 13:55–84
63. Mullay J (1987) Struct Bond 66:1–25
64. Sacher E, Currie JF (1988) J Electron Spectrosc Relat Phenom 46:173–177
65. Politzer P, Grice ME, Murray JS (2001) J Mol Struct THEOCHEM 549:69–76
66. Iczkowski RP, Margrave JL (1961) J Am Chem Soc 83:3547–3551
67. Parr RG, Donnelly RA, Levy M, Palke WE (1978) J Chem Phys 68:3801–3807
68. Gopinathan MS, Whitehead MA (1980) Israel J Chem 19:209–214
69. Nguyen-Dang TT, Bader RWF, Essen H (1982) Int J Quantum Chem 22:1049–1058
70. Parr RG, Yang W (1989) Density-functional theory of atoms and molecules. Oxford University Press, New York
71. Gázquez JL, Ortiz E (1985) J Chem Phys 82:5565–5570
72. Politzer P, Huheey JE, Murray JS, Grodzicki M (1992) J Mol Struct Theochem 259:99–120
73. Politzer P, Murray JS (2006) Chem Phys Lett 431:195–198
74. Politzer P, Murray JS, Concha MC, Jin P (2007) Collect Czech Chem Commun 72:51–63
75. Pearson RG (1990) Acc Chem Res 23:1–2

76. Allen LC (1990) Acc Chem Res 23:175–176
77. Allen LC (1989) J Am Chem Soc 111:9003–9014
78. Mann JB, Meek TL, Allen LC (2000) J Am Chem Soc 122:2780–2783
79. Mann JB, Meek TL, Knight ET, Capitani JF, Allen LC (2000) J Am Chem Soc 122:5132–5137
80. Lide DR (ed) (1997) Handbook of chemistry and physics, 78th edn. CRC Press, Boca Raton
81. Allred AL, Rochow EG (1958) J Inorg Nucl Chem 5:264–268
82. Politzer P, Murray JS, Grice ME (2005) Collect Czech Chem Commun 70:550–558
83. Bader RFW, Carroll MT, Cheeseman JR, Chang C (1987) J Am Chem Soc 109:7968–7979
84. Jameson CJ, Buckingham AD (1980) J Chem Phys 73:5684–5692
85. Bonin KD, Kresin VV (1997) Electric-Dipole polarizabilities of atoms, molecules and clusters. World Scientific, Singapore
86. Pearson RG (1963) J Am Chem Soc 85:3533–3539
87. Pearson RG (1993) Struct Bond 80:1–10
88. Huheey JE (1965) J Phys Chem 69:3284–3291
89. Huheey JE (1971) J Org Chem 36:204–205
90. Politzer P (1987) J Chem Phys 86:1072–1073
91. Politzer P, Huheey JE, Murray JS, Grodzicki M (1992) J Mol Struct Theochem 259:99–120
92. Ghanty TK, Ghosh SK (1993) J Phys Chem 97:4951–4953
93. Hati S, Datta D (1994) J Phys Chem 98:10451–10454
94. Símón-Manso V, Fuentealba P (1998) J Phys Chem A 102:2029–2032
95. Glasstone S (1940) Text-book of physical chemistry. Van Nostrand, New York
96. Teixeira-Dias JJC, Murrell JN (1970) Mol Phys 19:329–335
97. Dmitrieva IK, Plindov GI (1983) Phys Scr 27:402–406
98. Gough KM (1989) J Chem Phys 91:2424–2432
99. Brinck T, Murray JS, Politzer P (1993) J Chem Phys 98:4305–4306
100. Jin P, Murray JS, Politzer P (2004) Int J Quantum Chem 96:394–401
101. Fricke B (1986) J Chem Phys 84:862–866
102. Politzer P, Jin P, Murray JS (2002) J Chem Phys 117:8197–8202
103. Stott MJ, Zaremba E (1980) Phys Rev A 21:12–23
104. Vela A, Gázquez JL (1990) J Am Chem Soc 112:1490–1492
105. Jin P, Brinck T, Murray JS, Politzer P (2003) Int J Quantum Chem 95:632–637
106. Jin P, Murray JS, Politzer P (2006) Int J Quantum Chem 106:2347–2355
107. Politzer P, Murray JS, Grice ME (1993) Struct Bond 80:101–114
108. Parr RG, Pearson RG (1983) J Am Chem Soc 105:7512–7516
109. Bulat FA, Toro-Labbé A, Brinck T, Murray JS, Politzer P (2010) J Mol Model, in press (doi:10.1007/s00894-010-0692-x)
110. Scrocco E, Tomasi J (1978) Adv Quantum Chem 11:115–193
111. Politzer P, Daiker KC (1981) In: Deb BM (ed) The force concept in chemistry. Van Nostrand Reinhold, New York, ch 6
112. Politzer P, Murray JS (1991) In: Lipkowitz KB, Boyd DB (eds) Reviews in computational chemistry, Vol 2. New York, VHS, ch 7
113. Murray JS, Sen K (eds) (1996) Molecular electrostatic potentials: concepts and applicatons. Elsevier, Amsterdam
114. Brinck T, Murray JS, Politzer P, Carter RE (1991) J Org Chem 56:2934–2936
115. Brinck T, Murray JS, Politzer P (1991) J Org Chem 56:5012–5015
116. Murray JS, Brinck T, Politzer P (1992) J Mol Struct Theochem 255:271–281
117. Brinck T, Murray JS, Politzer P (1993) Int J Quantum Chem 48:73–88
118. Gross KC, Seybold PG, Peralta-Inga Z, Murray JS, Politzer P (2001) J Org Chem 66:6919–6925
119. Ma Y, Gross KC, Hollingsworth CA, Seybold PG, Murray JS (2004) J Mol Model 10:235–239
120. Politzer P, Murray JS, Concha MC (2002) Int J Quantum Chem 88:19–27
121. Russo N, Toscano M, Grand A, Mineva T (2000) J Phys Chem A 104:4017–4021
122. Bulat FA, Murray JS, Politzer P, in preparation
123. Toro-Labbé A, Jaque P, Murray JS, Politzer P (2005) Chem Phys Lett 407:143–146
124. Murray JS, Seminario JM, Politzer P, Sjoberg P (1990) Int J Quantum Chem, Quantum Chem Symp 38(S24):645–653
125. Clar E (1972) The aromatic sextet. Wiley, London
126. Murray JS, Abu-Awwad F, Politzer P (2000) J Mol Struct Theochem 501–502:241–250
127. Schmidt O (1938) Z Phys Chem 39:39
128. Daudel P, Daudel R (1949) Bull Soc Chim Biol 31:353
129. Pullman A, Pullman B (1955) Adv Cancer Res 3:117
130. Cromwell NH, Graff MA (1952) J Org Chem 17:414–425
131. Wiberg KB (1965) Rec Chem Prog 26:143
132. Charton M (1970) In: Zabicky J (ed) Chemistry of the alkenes, vol 3. New York, Wiley-Interscience, ch 10
133. Wiberg KB (1984) Acc Chem Res 17:379–386
134. Jackson JE, Allen LC (1984) J Am Chem Soc 106:591–599
135. Politzer P, Jayasuriya K (1986) J Mol Struct (Theochem) 135:245–252
136. Cavalieri E, Calvin M (1972) J Chem Soc Perkin 1:1253–1256
137. Clar E (1964) Polycyclic hydrocarbons, 1-2. Academic Press, New York
138. Saito R, Dresselhaus G, Dresselhaus MS (1998) Physical properties of carbon nanotubes. Imperial College Press, London
139. Ajayan PM (1999) Chem Rev 99:1787–1800
140. Harris PJF (1999) Carbon nanotubes and related structures. Cambridge University Press, Cambridge
141. Peralta-Inga Z, Murray JS, Grice ME, Boyd S, O'Connor CJ, Politzer P (2001) J Mol Struct Theochem 549:147–158
142. Politzer P, Murray JS, Lane P, Concha MC (2006) In: Balandin AA, King KL (eds) Handbook of semiconductor nanostructures and devices, Vol. 2. American Scientific Publishers, Los Angeles, Ch 7
143. Politzer P, Murray JS, Lane P, Concha MC (2006) In: Sokalski WA (ed) Molecular materials with specific interactions: modeling & design. Springer, London, Ch 5
144. Dinadayalene TC, Murray JS, Concha MC, Politzer P, Leszczynski J (2010) J Chem Theor Comp 6:1351-1357
145. Politzer P, Murray JS, Lane P, Concha MC, Jin P, Peralta-Inga Z (2005) J Mol Model 11:258–264
146. Xiao D, Bulat FA, Yang W, Beratan D (2008) Nano Lett 8:2814–2818
147. Peralta-Inga Z, Lane P, Murray JS, Boyd S, Grice ME, O'Connor CJ, Politzer P (2003) Nano Lett 3:21–28
148. Politzer P, Lane P, Murray JS, Concha MC (2005) J Mol Model 11:1–7
149. Bulat FA, Murray JS, Politzer P, unpublished
150. Ayers PW, Nagy A (2007) J Chem Phys 126:144108 (1-6)